Leading baryons at HERA

R. Sacchi[a] (on behalf of the H1 and ZEUS collaborations)

[a]University of Torino and INFN,
via P. Giuria 1, 10125 Torino, Italy

Recent results on leading baryon production in *ep* scattering from the ZEUS and H1 collaborations are presented and compared with different production models.

1. Introduction

A significant fraction of the HERA *ep* events have been found to contain a leading baryon (LB) carrying a large fraction x_L of the incoming proton energy ($x_L > 0.2$) but a small transverse momentum ($p_T \lesssim 0.7$ GeV) [1–3]. The production mechanism is not completely understood. Although a fraction of these LBs may result from the hadronization of the proton remnant, the t-channel exchange of colour singlet virtual particles is expected to contribute significantly. In this picture, the target proton fluctuates into a virtual meson-baryon state. The meson scatters with the projectile lepton, leaving a fast forward baryon in the final state.

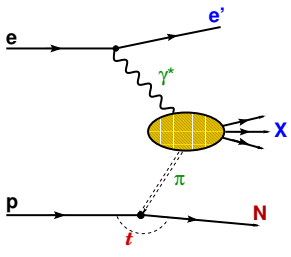

Figure 1. Leading neutron production via the pion exchange process.

In virtual exchange models, leading neutron (LN) production occurs through the exchange of isovector states, and π^+ exchange is expected to dominate (see figure 1). For leading proton (LP) production, isoscalar exchanges also contribute, including diffractive Pomeron mediated interactions.

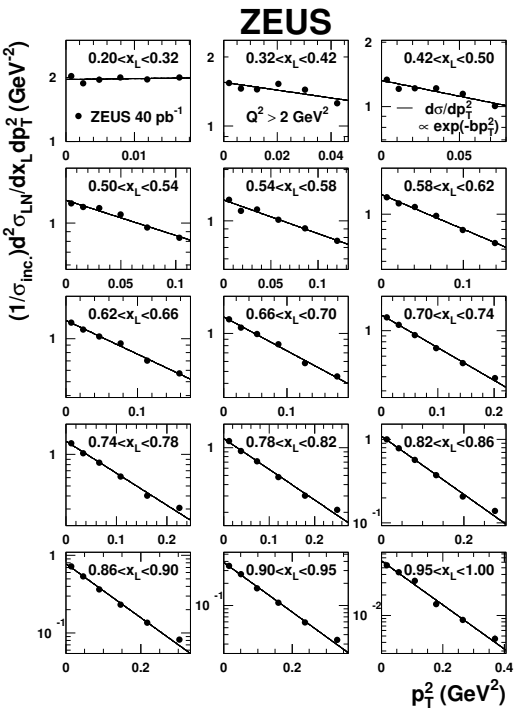

Figure 2. LN cross-section in DIS as function of p_T^2 in bins of x_L, normalized to the inclusive deep inelastic cross section. Lines are the results of fits to an exponential function.

In the simple exchange picture, the cross section is factorized and LB production is largely independent of the variables describing the photon vertex (vertex factorization). For example, if pion exchange dominates LN production, the cross section reads

$$d\sigma_{\gamma^* p \to nX} = f_{\pi/p}(x_L, t) \times d\sigma_{\gamma^* \pi \to X} \ .$$

Here $f_{\pi/p}$ is the flux of virtual pions in the proton, a universal factor constrained from low energy hadronic data, and $\sigma_{\gamma^*\pi\to X}$ is the $\gamma^*\pi$ cross section. Such a reaction can thus be used to probe the structure function F_2^π of the exchanged pion.

In the following, the results of two recent publications [4,5] of the ZEUS collaboration based on HERA-I measurements are presented, where the energy and the p_T distributions of LBs, shown both for photoproduction ($Q^2 < 0.02$ GeV^2) and deep inelastic scattering (DIS, $Q^2 \gtrsim 2$ GeV^2), are compared among themselves and to different production models. In addition, preliminary measurements of LN production in DIS by the H1 collaboration [6], based on the large statistics of the HERA-II data, are also shown; these measurements are used for the extraction of the pion structure function F_2^π.

2. Leading baryon production

Figure 2 shows the cross-section for LN production in DIS as a function of p_T^2 in bins of x_L, normalized to the inclusive DIS cross section. In each x_L bin the data are well described by an exponential distribution $a(x_L)\exp[-b(x_L)p_T^2]$.

The LN x_L distribution, the intercepts a and slopes b are compared in figure 3 to several Monte Carlo (MC) models [7,8]. None of the models incorporating only standard fragmentation predicts the observed LN yield, while `Lepto` with soft color interactions (SCI) [9] fails to describe the observed slopes. The `Rapgap` model, mixing standard fragmentation and π-exchange, gives a better description of the shape of the x_L distribution, and also predicts the rise of b with x_L, although with too high values.

A similar failure to describe the data is observed for LP production in DIS. Figure 4 (left) shows a comparison of the LP x_L distribution and

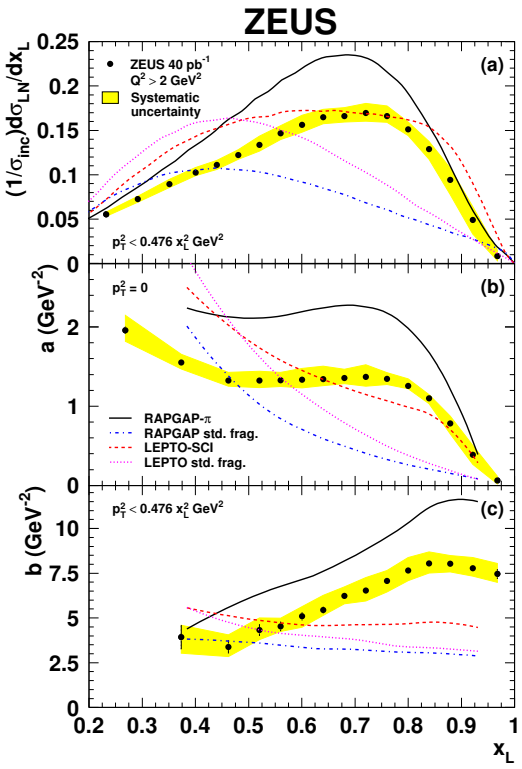

Figure 3. Normalized LN cross section, intercept a and exponential slope b of in DIS as function of x_L, compared to several Monte Carlo models.

the p_T^2 exponential slope b to the predictions of Monte Carlo models. None of them can reproduce either the flat dependence of the cross section versus x_L below the diffractive peak at $x_L = 1$ or the magnitude and dependence of b on x_L.

The same data are compared in figure 4 (right) to a Regge-based model [10] incorporating both isovector and isoscalar exchanges, including the Pomeron for diffraction. A good description of the x_L distribution and the slopes is obtained by adding a substantial contribution of isoscalar Reggeon exchanges, which turn out to be the dominant processes below the diffractive peak.

In the pure pion exchange model for LN production, the factorization relation discussed in

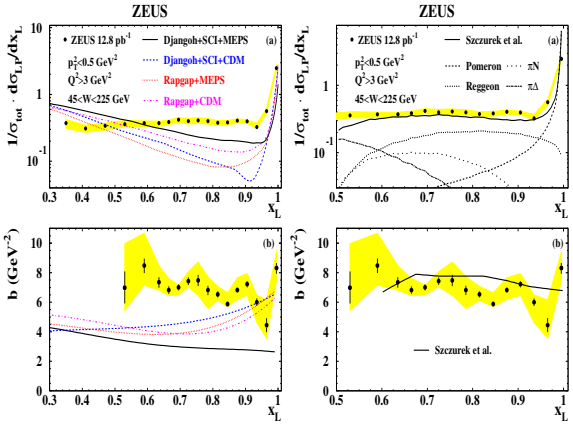

Figure 4. Normalized LP cross section and exponential slope b of LPs in DIS as function of x_L, compared to Monte Carlo models (left) and a Regge-based model [10] (right).

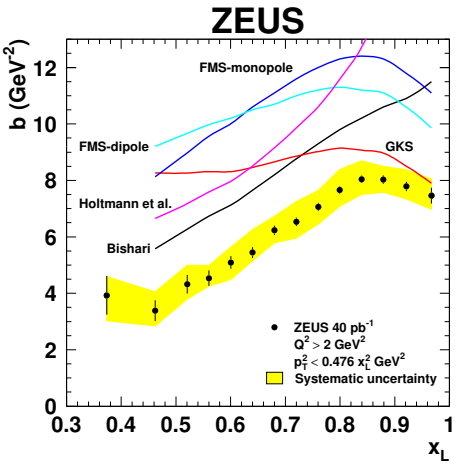

Figure 5. The measured exponential slopes b of LN production in DIS, compared to the predictions of models of one-pion exchange alone [11,12].

the introduction implies that, if $\sigma_{\gamma^*\pi}$ is assumed to be independent of t, the p_T^2 distribution solely depends on the pion flux factor $f_{\pi/p}$. The validity of the pure pion model can be tested by comparing the slopes b with various parametrizations of the pion flux. The results are shown in figure 5, where only the models that most resemble the data [11,12] have been retained for this comparison. All these models give values for the slopes larger than the data, suggesting that pion exchange alone is unable to describe the observed p_T^2 distributions.

3. Factorization breaking and absorption

A refinement of the simple factorization picture is provided by baryon absorption, which can occur through rescattering [13–15]. In a geometrical picture [14], if the size of the meson-baryon system is small compared to the size of the photon, the baryon may also scatter on the photon and migrate to lower x_L or higher p_T, thus escaping detection. This results in a relative depletion of observed forward baryons.

Since the size of the photon is inversely related to the photon virtuality Q^2, more absorption is expected in photoproduction ($Q^2 \simeq 0$) than in DIS, leading to a breaking of the vertex factorization.

Also, since the size of the meson-baryon system is inversely proportional to the baryon p_T, rescattering results in a depletion of high p_T baryons in photoproduction relative to DIS, again a violation of vertex factorization.

To investigate the Q^2 dependence of LN production, the x_L distributions for photoproduction and for DIS in three bins of increasing Q^2 are shown in figure 6. The yield of LNs decreases monotonically with decreasing Q^2, a clear violation of vertex factorization. This is in qualitative agreement with the expectations of an increase of absorption as Q^2 decreases. A similar Q^2 dependence of the yield, not shown here, is also observed in the LP data [4].

The Q^2 dependence of the p_T^2 distributions can be best examined by looking at the difference $\Delta b = b(Q^2 < 0,02\text{GeV}^2) - b(Q^2 > 2\text{GeV}^2)$ between the slopes of the exponential fits, described in the previous section, to the photoproduction

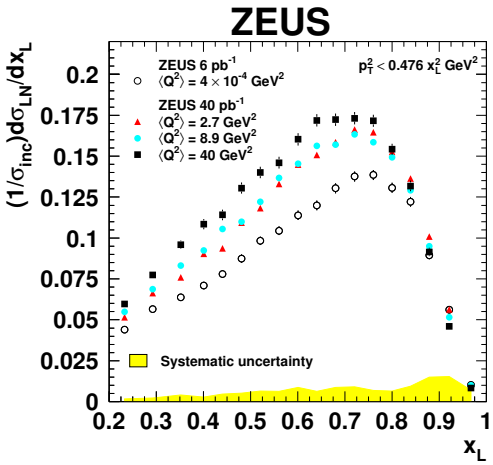

Figure 6. Normalized LN cross section as function of x_L for photoproduction and for three bins of Q^2 in DIS.

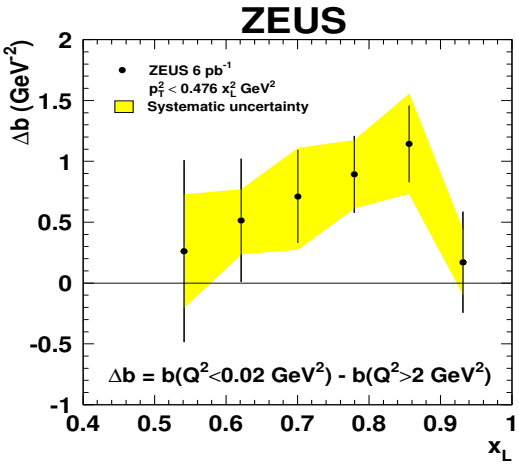

Figure 7. The differences between the exponential slopes in photoproduction and DIS, Δb, versus x_L.

and to the DIS p_T^2 distributions. This quantity is less sensitive to systematic effects than each individual slope and is shown in figure 7 for LN production as a function of x_L. The p_T^2 distributions are steeper (larger slope) in photoproduction than in DIS. This is consistent with the violation of vertex factorization discussed above, i.e. the absorption of large p_T neutrons in photoproduction leads to a larger slope than in DIS.

A calculation of LN production through pion exchange with neutron absorption, based on multi-pomeron exchanges, has become available [15]. It includes, in addition to the rescattering implemented in the earlier model [13], a small contribution from rescattering on the intermediate partons in the central rapidity region. It also accounts for the migration of the neutrons in x_L and p_T after rescattering and has been extended to include secondary exchanges of ρ and a_2 mesons.

The prediction of this model for the x_L neutron distribution in photoproduction, where rescattering is most important, is shown in figure 8, for pion exchange only, with a dashed curve. A fair description of both the shape and the magnitude

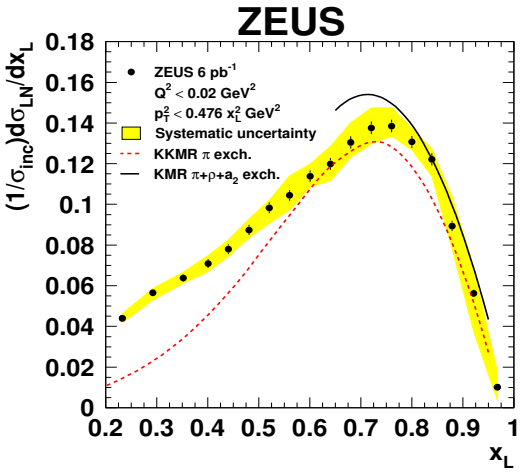

Figure 8. Normalized LN cross section as function of x_L in photoproduction. The curves represent the predictions of a model with neutron absorption and migration [15] for pion exchange only (dashed curve) and including ρ and a_2 exchanges (solid curve).

of the distribution is observed. However, as with the pure pion exchange discussed in the previous section, the model with pion exchange only predicts too high a value of the slope b, see figure 9(a). Extending the model to include also secondary exchanges (the solid curves in figures 8 and 9), a better description of the observed slopes is obtained still while maintaining a fair description of the x_L distribution. A reasonable description of the difference of the slopes Δb in photoproduction and DIS is also achieved, see figure 9(b).

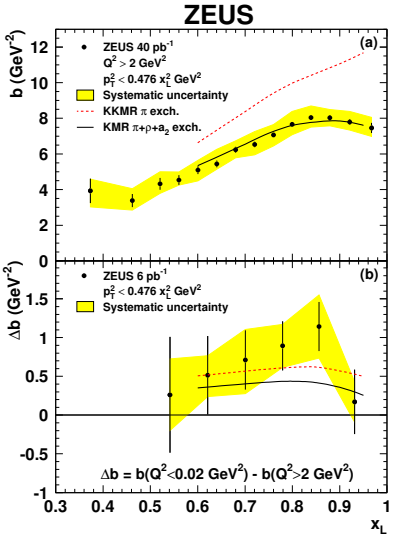

Figure 9. (a) Exponential slopes b for DIS and (b) difference of slopes b for photoproduction and DIS. The curves represent the predictions of a model with neutron absorption and migration [15] for pion exchange only (dashed curve) and including ρ and a_2 exchanges (solid curve).

Note that within this model, the present data can be used to constrain the gap-survival probability, one of the important inputs to calculations of diffractive interactions at the LHC [16].

4. The leading baryon and the pion structure functions

Analogous to the inclusive proton structure function $F_2(x, Q^2)$, the semi-inclusive LB structure function $F_2^{LB(3)}(x, Q^2)$ is defined which also includes dependence on x_L.

Figure 10 shows the ratios $F_2^{LN(3)}/F_2$ in bins of x and x_L as a function of Q^2, where F_2^{LN} values are measured from LN production in DIS, and F_2 is obtained from the H1-2000 parametrisations [17]. At fixed x_L, ratios are almost flat in all (x,Q^2) bins, suggesting the validity of factorization, i.e. independence of the photon and proton vertices.

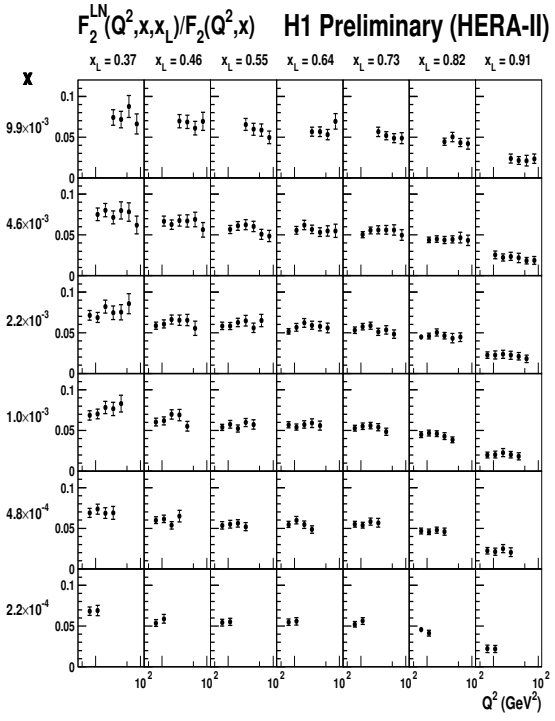

Figure 10. Ratio of the semi-inclusive structure function $F_2^{LN(3)}(Q^2, x, x_L)$ to the inclusive structure function $F_2(Q^2, x)$.

Similar behaviour is observed for LP production in DIS. The LP structure function $F_2^{LP(2)}(x, Q^2)$, integrated over an x_L range which excludes the diffractive region, is presented in figure 11. The data are compared to the inclusive F_2 obtained from the NLO ZEUS-S parametrisations [18] scaled by the average measured LP yield. A very good description of F_2^{LP} is observed, suggesting a fraction of DIS events containing LPs independent of x and Q^2, as expected by factorization.

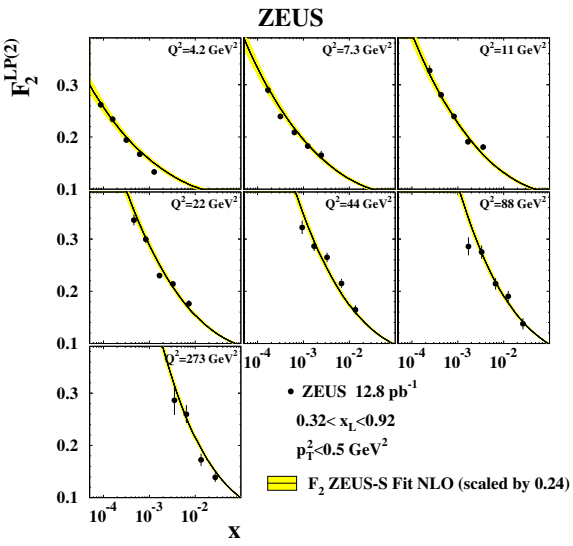

Figure 11. The semi-inclusive structure function $F_2^{LP(2)}(x, Q^2)$ in the kinematic range indicated in the figure. The curves show the F_2 parametrizations scaled by 0.24.

Assuming that the pion exchange mechanism dominates the LN production at large x_L, F_2^{LN} can be factorized into a product of a pion flux factor $f_{\pi/p}(x_L, t)$ times the pion structure function $F_2^{\pi}(\beta, Q^2)$, where $\beta = x/(1-x_L)$ is the fraction of the pion momentum carried by the struck parton.

The pion parton distributions have been previously constrained from Drell-Yan processes and direct photon production in pion-nucleon collisions, and are limited to high β ($\beta \gtrsim 0.1$) values.

Using the measurement of $F_2^{LN(3)}$ for $0.68 < x_L < 0.77$ and the integral over t of the pion flux factor [11] at the center of this x_L range, $\Gamma_\pi = \int f_{\pi/p} dt = 0.131$, the pion structure function can be extracted as $F_2^{\pi} = F_2^{LN}/\Gamma_\pi$.

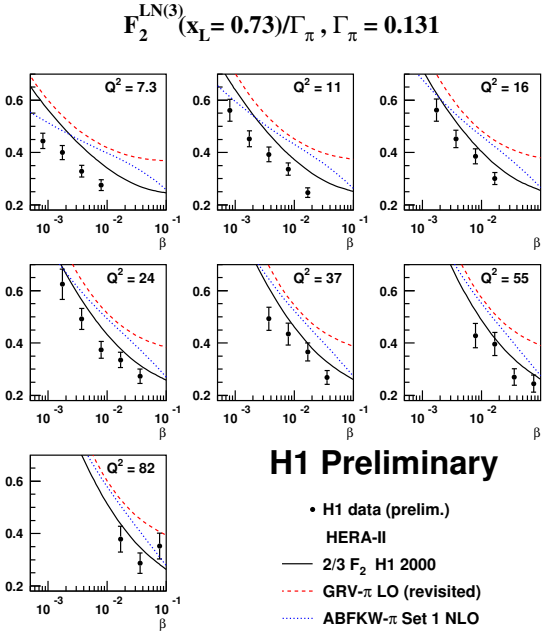

Figure 12. The pion structure function F_2^{π} as a function of β for fixed values of Q^2. The curves are the proton structure function scaled by 2/3 and two parametrizations of the pion structure function [19].

The result is shown in figure 12 as a function of β for fixed values of Q^2. The data are compared to the predictions of parametrisations of the pion structure function [19] as well as to the H1-2000 parametrisation of the proton structure function multiplied by the factor 2/3, according to the

naive expectation based on the number of valence quarks in the pion and the proton respectively. The measured data show a steep rise with decreasing β, in accordance with two F_2^π parametrisations, but are slightly below the expectations, suggesting that additional phenomena, like absorption, may play a role. Also, the theoretical uncertainties on the pion flux factor need to be carefully considered before any conclusion can be drawn. These results are also consistent with a previous ZEUS measurement [1].

REFERENCES

1. S. Chekanov *et al.* [ZEUS Collaboration], Nucl. Phys. B **637** (2002) 3.
2. C. Adloff *et al.* [H1 Collaboration], Eur. Phys. J. C **6** (1999) 587.
3. S. Chekanov *et al.* [ZEUS Collaboration], Nucl. Phys. B **658** (2003) 3.
4. S. Chekanov *et al.* [ZEUS Collaboration], preprint DESY 08-176 (2008), to be published in JHEP.
5. S. Chekanov *et al.* [ZEUS Collaboration], Nucl. Phys. B **776** (2007) 1.
6. H1 Collab., contribution to ICHEP08, H1prelim-08-111.
7. G. Ingelman, A. Edin and J. Rathsman, Comput. Phys. Commun. **101** (1997) 108.
8. H. Jung, Comput. Phys. Commun. **86** (1995) 147.
9. A. Edin, G. Ingelman and J. Rathsman, Phys. Lett. B **366** (1996) 371.
10. A. Szczurek, N.N. Nikolaev and J. Speth, Phys. Lett. B **428** (1998) 383.
11. H. Holtmann *et al.*, Phys. Lett. B **338** (1994) 363.
12. M. Bishari, Phys. Lett. B **38** (1972) 510;
    L.L. Frankfurt, L. Mankiewicz and M.I. Strikman, Z. Phys. A **334** (1989) 343;
    K. Golec-Biernat, J. Kwiecinski and A. Szczurek, Phys. Rev. D **56** (1997) 3955.
13. N.N. Nikolaev, J. Speth and B.G. Zakharov, preprint KFA-IKP(TH)-1997-17 (1997), hep-ph/9708290.
14. U. D'Alesio and H.J. Pirner, Eur. Phys. J. A **7** (2000) 109.
15. A.B. Kaidalov *et al.*, Eur. Phys. J. C **47** (2006) 385;
    V.A. Khoze, A.D. Martin and M.G. Ryskin, Eur. Phys. J. C **48** (2006) 797.
16. V.A. Khoze, A.D. Martin and M.G. Ryskin, Phys. Lett. B **643** (2006) 93.
17. C. Adloff *et al.* [H1 Collaboration], Eur. Phys. J. C **21** (2001) 33.
18. S. Chekanov *et al.* [ZEUS Collaboration], Eur. Phys. J. C **42** (2005) 13.
19. M. Glück, R. Reya and I. Schienbein, Eur. Phys. J. C **6** (1999) 313;
    P. Aurenche *et al.*, Phys. Lett. B **233** (1989) 517.